



## Numerical and Physical Investigation of the Mixing Process in Gas Stirred Ladle System

Sathaporn Lakkum, Patiparn Ninpetch, Nadnapang Phophichit and Pruet Kowitwarangkul\*

Department of Materials and Production Engineering, The Sirindhorn International Thai-German Graduate School of Engineering (TGGS), King Mongkut's University of Technology North Bangkok, Bangkok, Thailand

Atthasit Tawai

Department of Chemical and Process Engineering, The Sirindhorn International Thai-German Graduate School of Engineering (TGGS), King Mongkut's University of Technology North Bangkok, Bangkok, Thailand

Somboon Otarawanna

National Metal and Materials Technology Center (MTEC), National Science and Technology Development Agency (NSTDA), Pathum Thani, Thailand

\* Corresponding author. E-mail: pruet.k@tggs.kmutnb.ac.th DOI: 10.14416/j.asep.2020.07.001

Received: 18 March 2020; Revised: 20 May 2020, Accepted: 16 June 2020; Published online: 9 July 2020

© 2020 King Mongkut's University of Technology North Bangkok. All Rights Reserved.

### Abstract

Secondary steelmaking or ladle metallurgy is one of the important processes that adjust and homogenize the chemical compositions and the temperature. In this process, argon gas is injected into the melt through porous plugs to accelerate the chemical reaction and the mixing. One of the indicators for the mixing efficiency is “the mixing time”. The purposes of this study were to investigate the effects of gas flow rate and purging system on the mixing time and flow characteristics by using numerical and physical investigation and to predict the velocity magnitude acting on the refractory wall by analyzing the effects of gas flow rate. A 1:5 scaled water model and a full-scale ladle model of Millcon steel PLC were used in the study. The numerical simulation modelling was carried out by using CFD commercial software Flow-3D. The results from the numerical simulation were in consistence with the experiment results. The simulation results showed that with the highest gas flow rate the reduction of the mixing time was around 36% and the velocity magnitude increased to approximately 44% in comparison with the lowest gas flow rate in the full-scale model. The area at the ladle wall near the liquid surface has a higher chance of the damage than other areas. Besides, employing the dual-plugs system led to approximately 33–49% shorter mixing time compared to the single-plug system. The results show that the gas flow rate affects the turbulent kinetic energy directly. However, high turbulent kinetic energy leads to open-eye size which results in re-oxidation and contamination. Therefore, it is important to optimize the flow rate to achieve both productivity and steel cleanliness.

**Keywords:** Ladle metallurgy, Mixing time, Numerical simulation, Physical water model, Velocity magnitude

Please cite this article in press as: S. Lakkum, P. Ninpetch, N. Phophichit, P. Kowitwarangkul, A. Tawai, and S. Otarawanna, “Numerical and physical investigation of the mixing process in gas stirred ladle system,” *Applied Science and Engineering Progress*, (2020). DOI: 10.14416/j.asep.2020.07.001

## 1 Introduction

Secondary steelmaking or ladle metallurgy is the process that adjusts and controls the chemical compositions and the temperature as well as inclusion removal from the liquid steel. In this process, the argon gas is often injected into the liquid steel in order to stir and mix the chemical compositions until the homogeneity [1]. The time since the beginning of the stirring process until the point where the chemical compositions achieve the desired or specified degree of homogeneity is called “mixing time” [2]. Generally, the mixing time is fixed at 95%, which means the chemical compositions still remain within 5% of the final concentration [2], [3]. The typical variation of concentration with time and the procedure for estimating the 95% mixing time is shown in Figure 1.

It is well known that steel plants often reduce the mixing time by using higher gas flow rates. However, the high gas flow rate does not always provide good results. Lakkum *et al.* [4] illustrated the disadvantage of the excessive gas flow rate used in the ladle stirring process. The results indicated that the excessive flow significantly increases the turbulent kinetic energy, which results in the increasing of slag open-eye size and will promote the oxidation and contamination of inclusion in the liquid steel.

Over the past decades, the flow characteristics and the mixing phenomena in the gas stirred ladle system has been investigated widely by using the physical water model [5], [6] and numerical simulation [7], [8]. Many pieces of research give emphasis on the impact of injector design on mixing and flow characteristics. Owusu *et al.* [9] described the impact of six types of injector on mixing efficiency. They found that the standard porous plug provides higher intensive bulk convection and degree of turbulence than the other tested injectors. Gajjar *et al.* [10] also investigated the impact of six types of injector on mixing time, which correlates with the bulk convection and turbulent kinetic energy. The results indicated that the relative deviation in mixing time for all tested injectors is 6.4%. It can be concluded that the mixing time is independent of diameter orifices and the types of injector have a minor effect on the mixing efficiency.

While the numerical simulation has so far been applied in the ladle refining process. Mazumdar *et al.* [11] illustrated the combined Lagrangian-Eulerian approach to model the submerged gas injection

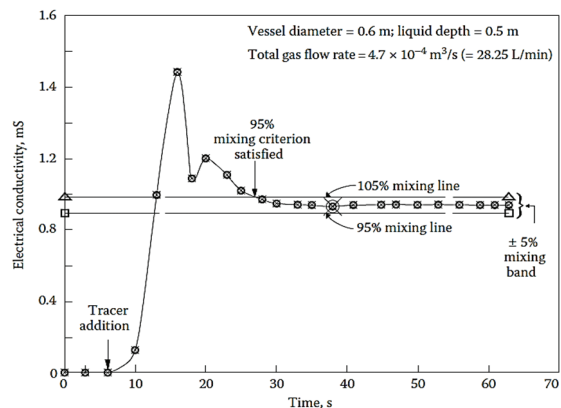


**Figure 1:** The variation of concentration with time and the procedure to estimate the 95% mixing time [1].

phenomena during ladle refining operations. The results provided the comprehension of the mathematical model which leads to the ladle stirred simulations. Madan *et al.* [12] presented the physical and mathematical modeling study to investigate the mixing in a gas stirred ladle system. The results exhibited that the comparison of mixing time between the discrete phase model (DPM) and the experimental measurements in general agree reasonably well. These prior research studies lead to a greater understanding of the simulation used in the gas stirred ladle system.

In this research, the objectives were divided into two parts. In the first part, the investigation of the effects of gas flow rate and purging system on the mixing time and flow characteristics were carried out by using numerical simulation, the commercial software, Flow-3D with experimental validation. A 1:5 scaled water model was applied in this part. In the second part, the effect of gas flow rates was investigated in order to predict the velocity magnitude acting on the refractory wall by using the numerical simulation. The full-scale ladle model of an example steel plant, Millcon Steel PLC was used in this part. This research attempted to show the importance of the optimisation of the gas flow rate inside the gas stirred ladle system which has direct effects on productivity and steel cleanliness.

## 2 Methodology

### 2.1 Physical modeling

Due to the difficulty of the measurement in the ladle



**Figure 2:** The 1:5 scaled water model station.

refining process such as the high temperature of the liquid steel, visual opacity of the liquid steel coupled with the large size of the industrial ladle furnace, the physical water model has been using to represent the system of the ladle refining process in order to study the phenomena in full-scale gas-stirred ladles. In this study, the main objectives of using the physical water model were to experimentally measure the mixing time as well as the tracer distribution inside the ladle.

The physical water model was scaled down 1:5 time of the actual ladle furnace nominal capacity of 75 tons from the example steel plant. Figure 2 shows the 1:5 scaled water model of the ladle used in the experiment. The physical water model and the water jacket were built by using transparent acrylic glass. The dimension of the 1:5 scaled water model and the full-scale ladle model are shown in Table 1.

**Table 1:** The ladle dimension of the 1:5 scaled water model and the full-scale ladle model

Properties	Full-scale Ladle Model (Steel-argon)	1:5 Scaled Water Model (Water-Air)	Unit
Ladle diameter (D)	2300	460	mm
Ladle height (H)	3000	600	mm
Liquid height (L)	2200	440	mm
Aspect ratio (L/2R)	0.9565	0.9565	-
Porous plug diameter	97	19.4	mm

As shown in Table 1, many research [13]–[16] mentioned the criteria of physical dimensions and operating parameters between the full-scale ladle system and the physical water model system. This

criterion is also known as Froude similarity criteria, which is derived on the basis of the effect of the gravity and the inertial force. The relationship of the gas flow rates between two different models can be represented as [Equation (1)]:

$$Q_{\text{mod}} = \lambda^{2.5} Q_{\text{fs}} \tag{1}$$

where  $Q_{\text{mod}}$  is gas flow rate in the model ( $\text{m}^3/\text{s}$ ),  $\lambda$  is geometrical scale factor ( $L_{\text{model}}/L_{\text{full-scale}}$ ), and  $Q_{\text{fs}}$  is gas flow rate in full-scale ladle ( $\text{m}^3/\text{s}$ ).

In the present study, the water was employed to represent the liquid steel and the upper slag phase is entirely ignored. The physical properties of the liquids and the operating conditions in the full-scale and the physical water model are summarized in Table 2.

**Table 2:** The physical properties of liquids used in the study [17]

Properties	Full-scale Ladle Model (Steel-argon)	1:5 Scaled Water Model (Water-Air)	Unit
Liquid density	6969	1000	$\text{kg}/\text{m}^3$
Liquid viscosity	0.0055	0.001	$\text{Pa}\cdot\text{s}$
Kinematic viscosity	$0.91 \times 10^{-6}$	$1 \times 10^{-6}$	$\text{m}^2/\text{s}$
Liquid temperature	1873	298	K
Injected gas	Argon	Compressed air	-
Gas density	1.6228	1.225	$\text{kg}/\text{m}^3$
Gas flow rate	100, 200, 300	1.8, 3.6, 5.4	$\text{L}/\text{min}$

## 2.2 Experimental setup

Figure 3 presents the schematic view of the experimental setup used to investigate the tracer distribution and the mixing time. The experimental system consists of water tap (1) to fill the water into the 1:5 scaled water model. The tracer was kept in the small container and injected into the water model by turning the ball valve (2). The tracer moved directly through the tracer inlet (3) to the point on the liquid surface. The movement of the tracer is moved independently according to the vertical axis. The characteristic of this movement is efficient to reduce the error due to the changing of the tracer velocity from the pouring. The gas injection system were set up to control pressure and air flow rate. The system consists of an air compressor (4), a pressure regulator (5) and a rotameter or flow meter (6). The gas was injected through the porous plugs (7) to generate

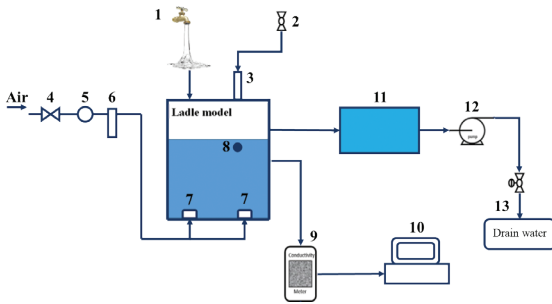


**Figure 3:** The schematic diagram of water modeling system setup used to analyze the tracer distribution and the mixing time.

the air bubble into the water. The conductivity probe (8) is located at 0.452 meters above the base of the ladle which used to measure the changing of the electrical conductivity from tracer (NaCl). The data was collected typically every one second and simultaneously stored in the conductivity meter (9) by using the Lutron Data Acquisition software. The data was converted and analyzed through the MS-Excel software in the computer (10). Then, the liquid in the water model is pumped out into a tank (11). The pump (12) pumped water out from the tank and the water was drained away as drain water (13).

However, there is little imprecision in the use of conductivity probe in the experimental study. Due to the complex shape of probe, which causes some obstruction of fluid flow in the conductivity sensor area, the 95% mixing time results in the experiment are higher than the results in the simulation which has no obstruction of fluid flow in the simulated probe. Accordingly, the adjustment of the mixing band in the concentration-time graph was increased from  $\pm 5\%$  to  $\pm 10\%$  to ignore the small fluctuation due to the obstruction of fluid flow in the experimental probe. For this reason, the 90% mixing time criterion was used in this study to indicate mixing phenomena that provide corresponding results in both simulation and experiment.

### 2.3 Mathematical models

The numerical simulation of mixing and flow in the gas stirred ladle system was primarily carried out by using the Lagrangian-Eulerian two-phase approach. In addition, the RNG k- $\epsilon$  model and the VOF model

were also applied in the simulation. The brief summary of the calculation procedures relevant to the present investigation is described as follows:

#### 2.3.1 Lagrangian-Eulerian two-phase approach or Discrete Phase Model

The combined models “Eulerian-Lagrangian” procedure by which the liquid flow and the turbulence are calculated on the Eulerian grid. The motion of bubbles with time in the liquid is calculated on the Lagrangian frame [1], [11]. In the simulation, a brief summary of the equations relevant to the present investigation is presented as follows:

Equations of continuity and momentum, the governing differential equations can be expressed as follows [18]:

Continuity Equation (2):

$$\nabla \cdot (u) = 0 \quad (2)$$

Momentum Equation (3):

$$\frac{\partial \rho u}{\partial t} + \nabla \cdot (\rho u u) = -\nabla p + \nabla \mu \nabla u \quad (3)$$

Where  $u$  is velocity,  $\rho$  is density,  $p$  is pressure, and  $\mu$  is dynamic viscosity.

Equations of bubble motion and bubble trajectory, the equations can be expressed as follows [19] [Equation (4)]:

$$\frac{du_p}{dt} = -\frac{1}{\rho_p} \nabla P + g + \beta(u - u_p) \left| u - u_p \right| \cdot \frac{\rho}{\rho_p} + \frac{m_{added}}{m_p} \left( \frac{du}{dt} - \frac{du_p}{dt} \right) \quad (4)$$

Where  $u_p$  is particle mean velocity,  $\rho$  is density,  $g$  is gravity and other body forces,  $u$  is fluid velocity,  $p$  is pressure,  $\beta$  is coefficient related to drag force,  $m_p$  is particle mass, and  $m_{added}$  is the added fluid mass.

#### 2.3.2 Renormalized group (RNG) k-epsilon model

The Renormalized Group (RNG) k- $\epsilon$  model is a more robust version of the two-equation k- $\epsilon$  model, and is recommended for most industrial problems. It extends

the capabilities of the standard k-ε model to provide better coverage of transitionally-turbulent flows, curving flows, wall heat transfer, and mass transfer. The equations can be expressed as follows [20] [Equation (5)]:

Turbulent kinetic energy, k:

$$\frac{\partial}{\partial t}(\rho k) + \frac{\partial}{\partial x_i}(\rho k u_i) = \frac{\partial}{\partial x_j} \left[ \left( \mu + \frac{\mu_t}{\sigma_k} \right) \frac{\partial k}{\partial x_j} \right] + P_k - \rho \varepsilon \quad (5)$$

The rate of dissipation of turbulent kinetic energy, ε [Equation (6)]:

$$\frac{\partial}{\partial t}(\rho \varepsilon) + \frac{\partial}{\partial x_i}(\rho \varepsilon u_i) = \frac{\partial}{\partial x_j} \left[ \left( \mu + \frac{\mu_t}{\sigma_\varepsilon} \right) \frac{\partial \varepsilon}{\partial x_j} \right] + \frac{\varepsilon}{k} [C_1 P_k - C_2 \rho \varepsilon] \quad (6)$$

### 2.3.3 Volume of fluid model (VOF model)

In this study, the VOF model was used to represent the interface behaviors of top liquid surface and gas layer in the gas stirred ladle system. The equation describes the volume fraction can be expressed below [21] [Equation (7)]:

$$\frac{\partial F}{\partial t} + u \frac{\partial F}{\partial x} = 0 \quad (7)$$

Where *F* is the fraction of the different phase

However, according to the mathematical models as mentioned above. It is required some assumptions in order to set the scope of the research and to ease the complexity of establishing the numerical simulation. The assumptions applied in this research are shown as follows:

- 1) The temperature in both systems was assumed isothermal in which the temperature remains constant.
- 2) The flow system is essentially turbulent and transient, which means the concentration at any location changes with time till the tracer concentration homogeneous.
- 3) The presence of an upper slag layer phase was

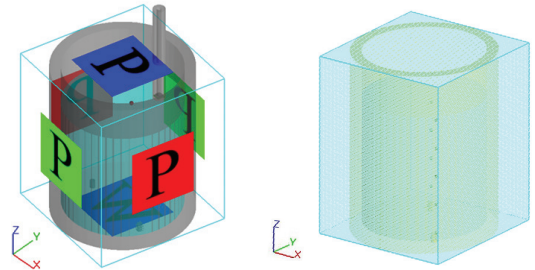


**Figure 4:** The 3D models of the ladle model: (a) Boundary conditions and (b) Meshing model.

ignored and the bulk liquid-air interface was set as a sharp interface.

4) The discrete bubbles were set to form at the porous plugs. The size of the bubble forming at the porous plug is defined as follows [21] [Equation (8)]:

$$d_b = 0.35 \left( \frac{Q^2}{g} \right)^{0.2} \quad (8)$$

Where *d<sub>b</sub>* is bubble diameter, *Q* is gas flow rate corrected to mean height and temperature of the liquid (m<sup>3</sup>/s), and *g* is gravitational acceleration (m/s<sup>2</sup>). The size of a bubble was estimated on the basis of the gas flow rate and was dynamically adjusted pressure and size of gas particles in response to pressure in the surrounding fluid.

5) The interactions between bubble-bubble were ignored.

6) The standard drag law for spherical shape of bubble was applied in the simulation.

### 2.4 Computational conditions

Figure 4 shows the boundary conditions and the meshing model of the gas stirred ladle simulation. Both full-scale ladle and 1:5 scaled water model use similar boundary conditions which consist of specified pressure (P) and wall (W). The atmospheric pressure at 1.01325×10<sup>5</sup> Pa was set up at the top and the side wall. The standard wall function with non-slip condition was set at the bottom wall. Additionally, the boundary conditions at the tracer inlet, porous plugs, and liquid surface were specified. For the meshing model, both ladle models used one mesh block. The computational mesh to solve the discrete and continuous phase equations consists of approximately 704,238 cells.

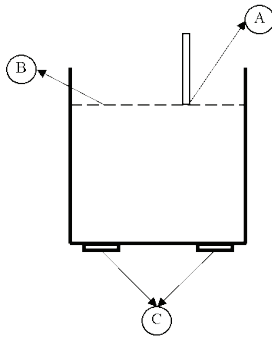


**Figure 5:** The boundary conditions at (A) tracer inlet, (B) liquid surface and (C) porous plugs.

From Figure 5, at the tracer inlet (position A), a pulse tracer addition is injected into the liquid with a fixed velocity for two seconds. At the liquid surface (position B), the bubbles can be escaped through the liquid surface. Finally, the sizes of the bubble are defined according to the different gas flow rates at the porous plugs (position C).

### 3 Results and Discussion

#### 3.1 Effects of gas flow rate and purging system on the mixing time

Figure 6 illustrates the arrangement inside both the full-scale ladle model and the 1:5 scaled water model used in this part. In Table 3, mixing time from the simulation results were validated with experiment results. It is readily evident that the results from the numerical simulation are in consistent with the experiment results. It shows that the gas flow rate affects the mixing time directly. The results indicated that by increasing the gas injection, the mixing time is decreased. This can be explained by the fact that the injection of gas flow rate into the liquid steel promotes the stirring and the recirculation flow inside the ladle, which accelerate the chemical composition to homogeneous. When comparing the two systems, it was discovered that with the same position of the probe, the mixing time with both single-plug systems is slower than that of dual-plugs system. The results exhibited that the number of the porous plugs significantly affect the 90% mixing time. At this point, it can be summarized that the dual-plugs system provides better mixing efficiency than the single-plug system. The simulation results of the full-scale ladle model shown in Table 4 present the effects of gas flow

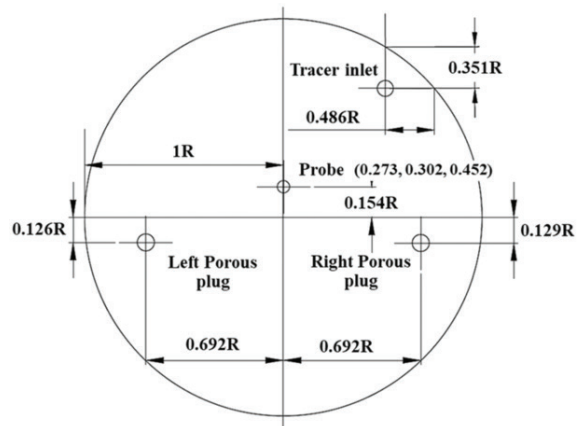


**Figure 6:** The arrangement of the tracer adding point, the conductivity probe and the porous plugs with divided porous plugs into left and right plug.

rates, numbers and positions of porous plug, and the tracer adding point on 90% mixing time which have similar trend to that of the 1:5 scaled water model.

**Table 3:** The comparison of simulation results and experimental results of dual-plugs and single-plug systems of the 1:5 scaled water model

Purging Systems	Gas Flow Rate (L/min)	90% Mixing Time (s)	
		Experiment	Simulation
Dual-plugs	1.8	40	45
	3.6	34	38
	5.4	30	32
Single-plug (Right)	1.8	67	70
	3.6	55	59
	5.4	45	48
Single-plug (Left)	1.8	75	78
	3.6	65	68
	5.4	57	60

**Table 4:** The 90% mixing time of dual-plugs and single-plug from simulation results in the full-scale ladle model

Purging Systems	Gas Flow Rate (L/min)	90% Mixing Time (s)
		Simulation
Dual-plugs	100	115
	200	100
	300	80
Single-plug (Right)	100	160
	200	140
	300	120
Single-plug (Left)	100	170
	200	150
	300	132

From the Table 4, the reduction rate of mixing time in dual-plugs system illustrates that when increasing the gas flow rate from 100 to 200 L/min, a 115 s mixing time was brought down to 100 seconds (14%), and from 200 to 300 L/min, it was further brought down to 80 seconds (22%). In addition, the increasing of gas flow rate from 100 to 300 L/min results in a decrease in mixing time from 115 to 80 s (36%). The simulation results show that the reduction in mixing time is controlled by the gas flow rate. From the results of both ladle models, it can be concluded that the increase in gas flow rate results in mixing efficiency in gas-stirred ladle system. From the comparison results of single-plug and dual-plug purging systems, at the same gas flow rates of 100, 200, and 300 L/min, the mixing time rates were brought down about 33–39%, 33–40%, and 40–49%, respectively. These results state that the dual-plug system offers better mixing efficiency than the single-plug system under the same total flow rate conditions.

However, when comparing between the left and the right plug of the single-plug systems, an interesting finding is that the tracer adding point directly affects the mixing time. The results from both ladle models indicated that the mixing time from the right plug case is faster than the left plug case. This is because the tracer adding point is located closer to the right plug than the left plug as shown in Figure 6. At the area near the purging plug, there is high turbulent kinetic energy, which promotes the stirring efficiency and results in a decrease in the mixing time. This result is corresponding to the previous finding of Zhu [22].

### 3.1.1 Effects of positions of the probe on the mixing time

In the study of the effects of positions of the probe, the arrangement of the probes was changed from Figure 6 to Figure 7. The position of the probe can not be located close to the purging plug area as the bubble can disturb the measurement. The experiment and the simulation were carried out by using the 1:5 scaled water model in the dual-plugs system. The results are described as follows:

As shown in Table 5, it can be seen that the results from the simulation and the experiment are in good agreement. Only minor differences around 6–13% was found due to the small asymmetry and imprecision of the positions of the purging plug and conductivity

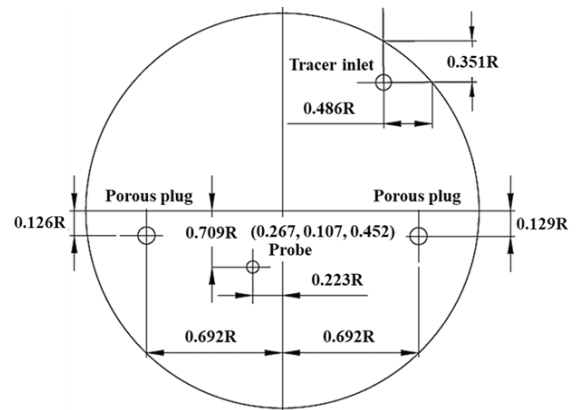


**Figure 7:** The arrangement of the probe after changed positions.

probe. The results show that the 90% mixing time of the new position is slower than the results of its original position. The mixing time after changing the probe positions are retarded as the new position is located near the affected region of the rising plume flow of porous plug. Thus, it can be concluded that the change in probe positions is sensitive to the mixing time.

**Table 5:** The comparison results of the effect of probe positions from the simulation and the experimental of the dual-plugs system of the 1:5 scaled water model

Purging system	Gas flow rate (L/min)	90% Mixing time (s)			
		Before changed		After changed	
		Exp	Sim	Exp	Sim
Dual-plugs	1.8	40	45	46	50
	3.6	34	38	40	43
	5.4	30	32	34	37

### 3.2 Effects of gas flow rate and purging system on the flow characteristics

The simulation shows similar prediction results of both models. To present the flow characteristics in the ladle which represent the actual phenomena inside the ladle of the example plant, the full-scale model is therefore chosen to present the effect of gas flow rate and purging system on the turbulent kinetic energy, the velocity flow field and the velocity streamlines in this part.

#### 3.2.1 The turbulent kinetic energy

Figure 8 shows the 2D turbulent kinetic energy at the

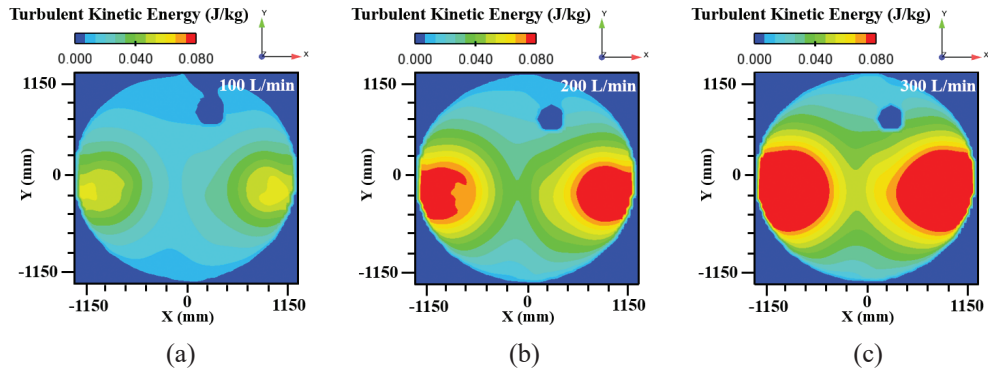


**Figure 8:** The turbulent kinetic energy with different gas flow rates in dual-plugs system of the full-scale ladle model: (a) 100 L/min, (b) 200 L/min, and (c) 300 L/min (The blue circle is the position of the tracer inlet).

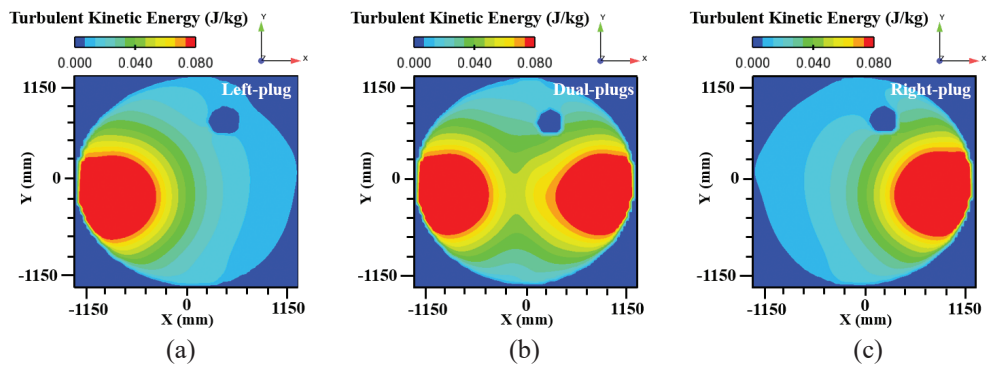


**Figure 9:** The turbulent kinetic energy at 300 L/min with different purging systems system of the full-scale ladle model: (a) Left-plug, (b) Dual-plugs, and (c) Right-plug (The blue circle is the position of the tracer inlet).

liquid surface of the full-scale ladle model, respectively. It can be seen that the trend of the results in both ladle models is similar. The results indicate that the increase of the gas flow rates subsequently increase the turbulent kinetic energy which affects the mixing time directly. The turbulent kinetic energy of the full-scale ladle model at the highest gas flow rates of 300 L/min are illustrated in Figure 9. The results show that, as there are two plumes region in the dual-plugs system, it can be obviously seen that there is larger area of turbulent kinetic energy than the single-plug system. In addition to the comparison of the turbulent kinetic energy areas of both systems, it was found that the maximum turbulent kinetic energy occurs in the middle of the plume region due to a large group of bubbles. The areas of the turbulent kinetic energy distribution are expanded and gradually decreased from the center of the plume regions.

However, high turbulent kinetic energy does

not always provide good results on the mixing. The contamination of the liquid steel can occur in ladles when open-eye area is expanded due to the increase of turbulent kinetic energy. As shown in Figures 8 and 9, it can be concluded that the gas flow rate should be optimized in order to improve the cleanliness quality of the liquid steel by decreasing the turbulent kinetic energy. It should be noted that the optimum limit value of turbulent kinetic energy for avoiding the problem of contamination can not be indicated from this study, but it is interesting for future work.

### 3.2.2 The velocity flow field

The simulation results of velocity flow field with different gas flow rates inside the ladle in Figure 10 show that the liquid velocity of the entire ladle is increased when increasing the gas flow rate. The increasing of the flow velocity has a direct influence on



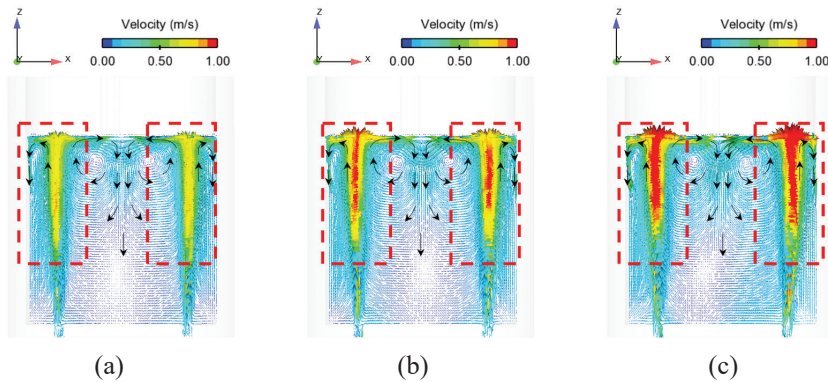


**Figure 10:** The velocity flow field with different gas flow rates in dual-plugs system of the full-scale ladle model: (a) 100 L/min, (b) 200 L/min, and (c) 300 L/min.

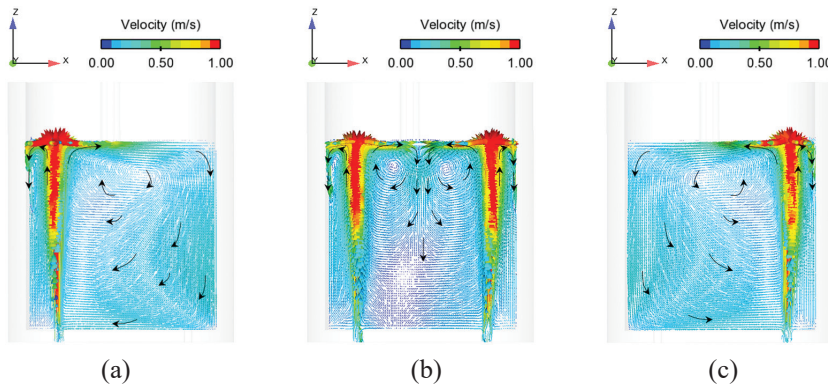


**Figure 11:** The velocity flow field at 300 L/min with different purging systems of the full-scale ladle model: (a) Left-plug, (b) Dual-plugs, and (c) Right-plug.

the mixing efficiency. The plume regions are formed and floated upward, then expanded to the liquid surface as illustrated in the red square frame. Intensive plume regions with high velocity value of the upward flow are caused by higher gas flow rates. However, higher velocity value can generate the open-eye on the surface of the liquid (Figures 8 and 9), which may cause contamination to liquid steel. Figure 11 shows the velocity flow field with different purging systems inside the full-scale ladle model. The flow field characteristics changes due to the different of purging systems which can be explained that the velocity flow field characteristics are significantly affected by the numbers of the porous plug.

### 3.2.3 The velocity streamlines

The comparison of the 3D velocity streamlines distribution inside the full-scale ladle model are shown in Figure 12.

The simulation results of both models indicated that when gas flow rates increase, the velocity of each path line is increased. The recirculation fluid-flow pattern is generated by gas injection through the porous plugs located at the bottom base. The flow characteristics can be divided into two patterns: an upward flow and a downward flow. The upward flow driven by the gas flow rates flows down from the top of the surface from both sides of the porous plugs before forming the downward flow. Figure 13 illustrates the comparison of the fluid-flow pattern between dual-plugs and single-plug of the full-scale ladle models. The results showed that the fluid-flow pattern inside the ladle changed due to the changing of the purging systems. It can be seen that the dual-plugs system causes a large circulation flow from both sides of the porous plugs while the single-plug generates a different flow pattern. From this point, it can be summarized that the number and

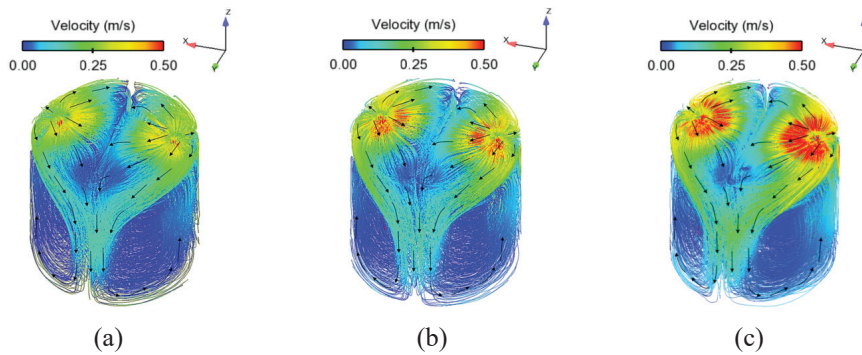


**Figure 12:** The velocity streamlines with different gas flow rates in dual-plugs system of the full-scale ladle model: (a) 100 L/min, (b) 200 L/min, and (c) 300 L/min.

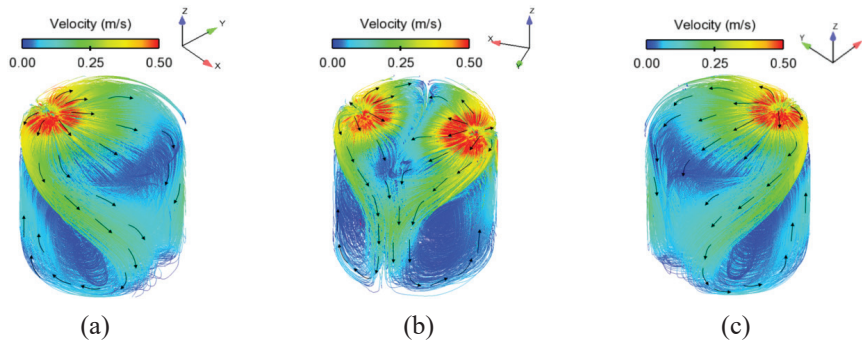


**Figure 13:** The velocity streamlines with different purging systems of the full-scale ladle model: (a) Left-plug, (b) Dual-plugs, and (c) Right-plug.

the position of porous plugs have significant effects on the fluid-flow pattern in the ladle.

### 3.3 Effects of gas flow rate on the velocity magnitude acting on the refractory wall

In this research, the velocity magnitude acting on the refractory wall is used as an indicator to represent the probability of the erosion occurred at the wall of ladle. The study was carried out by using the full-scale ladle model to predict the velocity magnitude. The arrangement inside the ladle is shown in Figure 6. In order to measure the velocity magnitude acting on the refractory wall, the probe must be fixed at the wall of the ladle. The positions of the probe are located vertically near the porous plugs on each side of the ladle wall. Thus, in this study, the arrangement of the probe to measure the velocity magnitude is determined as shown in Figure 14. The lowest probes are located 0.3 meters above the base of the ladle. The following

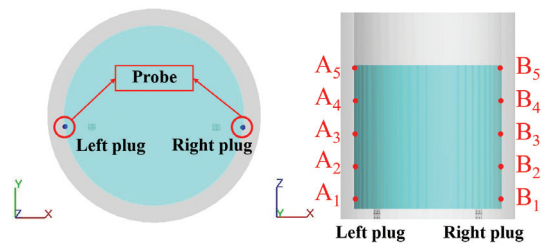


**Figure 14:** The arrangement of the probes to measure the velocity magnitude at the ladle wall of the full-scale ladle model: (a) Top view and (b) Side view.

probes are located above the lastest probe with the incremental scale of 0.5 meters. The results can be described as follows:

Figures 15–17 presents the velocity magnitude acting on the refractory wall according to the different gas flow rates of 100, 200, and 300 L/min, respectively. The results showed that the level of the velocity magnitude is accelerated with the increased gas flow rate. Similar

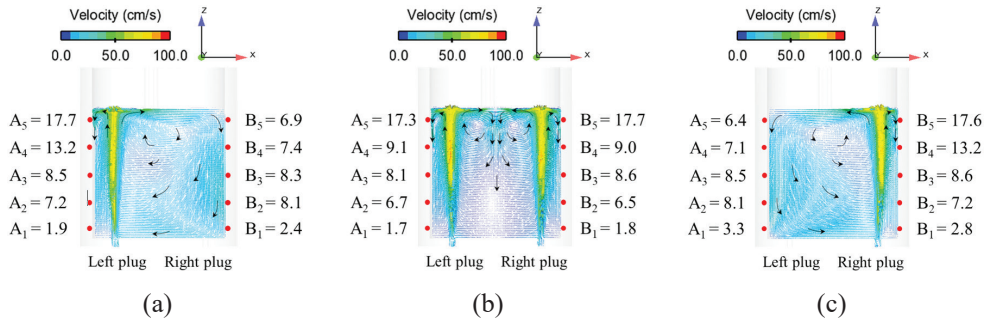


**Figure 15:** The velocity magnitude with different purging systems at 100 L/min: (a) Left-plug, (b) Dual-plugs, and (c) Right-plug.

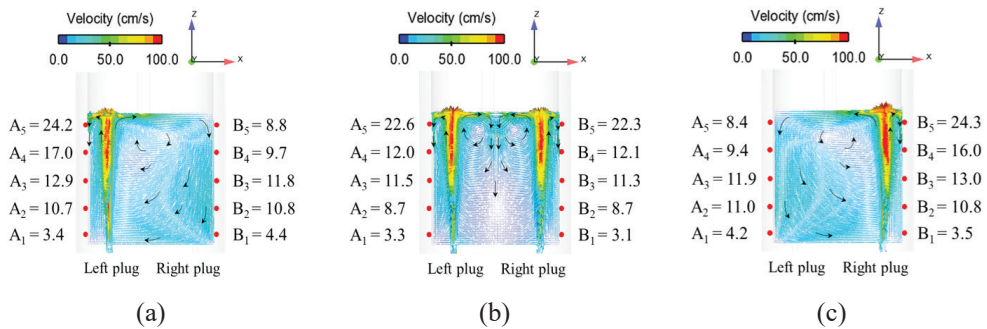


**Figure 16:** The velocity magnitude with different purging systems at 200 L/min: (a) Left-plug, (b) Dual-plugs, and (c) Right-plug.

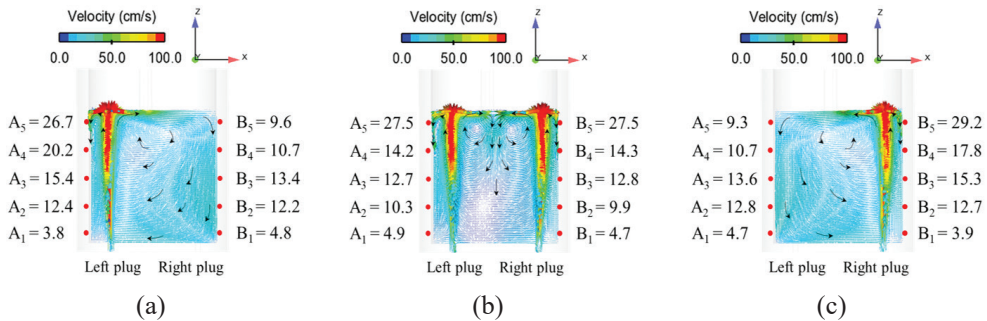


**Figure 17:** The velocity magnitude with different purging systems at 300 L/min: (a) Left-plug, (b) Dual-plugs, and (c) Right-plug.

to the study of A. Huang *et al.* [23], the higher erosion rate increases obviously with the increase of gas flow rate. In the dual-plugs system, the results of this current study show that the highest level of velocity magnitude occurred at A5 and B5, the probe point located near the liquid steel surface on the ladle wall with every gas flow rate when compared to the other points. Increasing the gas flow rates from 100 to 200 L/min, 200 to 300 L/min, and 100 to 300 L/min at the highest

probe point (A5 and B5), resulted in the increase in velocity magnitude to approximately 25, 20, and 44%, respectively.

In the single-plug system, the highest value of the velocity magnitude occurred at the highest probe point in the area of the lining near the purging plug. On the other hand, the other side of the ladle wall does not have a direct effect from the gas flow rate but is still affected from the recirculation flow of the liquid

steel inside the ladle. The results from the current study show that in the area of the lining wall near the liquid steel surface at the purging plug has higher chances of damages, which lead to the erosion of the refractory wall, from the gas stirring than the other areas.

#### 4 Conclusions

The first part of this study aimed to investigate the impact of the process parameters namely the gas flow rates, the numbers and positions of porous plugs, and the positions of the probe in order to predict the 90% mixing time. The study was investigated experimentally in a 1:5 scaled physical water model and validated with the numerical simulation. The results from the numerical simulation are in consistence with the experiment results. Both results show that the gas flow rate has a significant effect on the mixing time. In the full-scale model, the mixing time at the highest value of gas flow rate was approximately 36% shorter than the lowest one. The increase of gas flow rate directly affects the fluid-flow velocity and the turbulent kinetic energy in the entire ladle. The high turbulent kinetic energy enhances the probability of the open-eye are at the liquid surface, which results in re-oxidation and slag entrainment on the liquid surface. The results also reveal that numbers and positions of porous plugs have significant influence on the mixing time. The changing of purging systems from single-plug to dual-plugs reduces mixing time in all cases. The changing purging system directly affect the fluid-flow pattern, which affects the velocity flow field and pattern of velocity streamlines. Moreover, the mixing time is sensitive to the positions of the probe. When the probe is located near the rising bubble plume, the mixing time is retarded.

In the second part, the effect of different gas flow rates was investigated by using numerical simulation in order to predict the velocity magnitude acting on the refractory wall. The study was carried out by using a full-scale numerical ladle model which applied the geometric properties of the actual model at Millcon Steel PLC. The findings show that the velocity magnitude tends to increase when the gas flow rate is increased. The highest level of velocity magnitude occurred near the liquid surface which is a result from the effect of backward flow acting on the refractory wall. For this

reason, the area at the ladle wall near the liquid surface has higher chances of damages than the other areas. Increasing the gas flow rates from 100 to 200 L/min, 200 to 300 L/min, and 100 to 300 L/min at the highest probe point (A5 and B5), resulted in the increase in velocity magnitude to approximately 25, 20, and 44%, respectively. The results shows both advantages and disadvantages of using high gas flow rates. By increasing the gas flow rates, the mixing time is decreased and the turbulent kinetic energy is increased. However, high turbulent kinetic energy can expand open-eye size which results in re-oxidation and the contamination of the liquid steel. Therefore, it is important for the steel plant to optimize the gas flow rate in order to achieve both productivity and quality of the liquid steel product.

#### Acknowledgments

This research was funded by King Mongkut's University of Technology North Bangkok, Contract no. KMUTNB-62-DRIVE-36, Millcon Steel PLC, and the software license support from Flow Science, Inc and Design Through Acceleration Co., Ltd

#### References

- [1] D. Mazumdar and J. W. Evans, *Modeling of Steelmaking Processes*. Florida: CRC Press, 2009, p. 493.
- [2] H. M. Issa, "Power consumption, mixing time, and oxygen mass transfer in a gas-liquid contactor stirred with a dual impeller for different spacing," *Journal of Engineering*, vol. 2016, pp. 1–7, 2017.
- [3] D. Mazumdar and R. I. L. Guthrie, "The physical and mathematical modelling of gas stirred ladle systems," *ISIJ International*, vol. 35, no. 1, pp. 1–20, 1995.
- [4] S. Lakkum and P. Kowitwarangkul, "Numerical investigations on the effect of gas flow rate in the gas stirred ladle with dual plugs," in *IOP Conference Series: Materials Science and Engineering*, 2019, vol. 526, pp. 1–5.
- [5] J. Mandal, S. Patil, M. Madan, and D. Mazumdar, "Mixing time and correlation for ladles stirred with dual porous plugs," *Metallurgical and Materials Transactions B*, vol. 36, no. 4, pp. 479–487, 2015.
- [6] K. M. A. Ali, "Parameters influence on mixing time of gas liquid agitation system," *Journal of*

- Babylon University/Engineering Sciences*, vol. 22, no. 2, pp. 403–412, 2014.
- [7] F. Karouni, B. P. Wynne, J. T.-Silva, and S. Phillips, “Modeling the effect of plug positions and ladle aspect ratio on hydrogen removal in the Vacuum Arc Degasser,” *Steel Research International*, vol. 89, no. 5, pp. 1–8, 2018.
- [8] S. Torres and M. A. Barron, “Numerical simulation of an argon stirred ladle with top and bottom injection,” *Open Journal of Applied Science*, vol. 6, no. 13, pp. 860–867, 2018.
- [9] K. B. Owusu, T. Haas, P. Gajjar, M. Eickhoff, P. Kowitwarangkul, and H. Pfeifer, “Interaction of injector design, bubble size, flow structure, and turbulence in ladle metallurgy,” *Steel Research International*, vol. 90, no. 2, pp. 1–10, 2018.
- [10] P. Gajjar, T. Haas, K. B. Owusu, M. Eickhoff, P. Kowitwarangkul, and H. Pfeifer, “Physical study of the impact of injector design on mixing, convection and turbulence in ladle metallurgy,” *Engineering Science and Technology, an International Journal*, vol. 22, no. 2, pp. 538–547, 2018.
- [11] D. Mazumdar and R. I. L. Guthrie, “An assessment of a two phase calculation procedure for hydrodynamic modelling of submerged gas injection in ladles,” *ISIJ International*, vol. 34, no. 5, pp. 384–392, 1994.
- [12] M. Madan, D. Satish, and D. Mazumdar, “Modeling of mixing in ladles fitted with dual plugs,” *ISIJ International*, vol. 45, no. 5, pp. 677–685, 2005.
- [13] D. Mazumdar, H. B. Kim, and R. I. L. Guthrie, “Modelling criteria for flow simulation in gas stirred ladles: Experimental study,” *Ironmaking and Steelmaking*, vol. 27, no. 4, pp. 302–309, 2000.
- [14] D. Mazumdar, P. Dhandapani, and R. Sarvanakumar, “Modeling and optimisation of gas stirred ladle systems,” *ISIJ International*, vol. 57, no. 2, pp. 286–295, 2017.
- [15] D. Mazumdar, G. Yamanoglu, R. Shankarnarayanan, and R. I. L. Guthrie, “Similarity considerations in the physical modelling of steel making tundish systems,” *Steel Research International*, vol. 66, no. 1, pp. 14–19 1995.
- [17] P. Kowitwarangkul, M. Kamonrattapisud, E. Juntarasaro, and D. Sukam, “CFD simulation of molten steel flow with isothermal condition in continuous casting tundish,” *King Mongkut’s University of Technology North Bangkok International Journal of Applied Science and Technology*, vol. 9, no. 2, pp. 71–77, 2016.
- [18] N. Hasan, “Validation of CFD models using FLOW3D for a submerged liquid jet,” presented at the Ninth International Conference on CFD in the Minerals and Process Industries, Melbourne, Australia, Dec. 10–12, 2012.
- [19] *FLOW-3D*. Flow Science, Inc. Accessed: Mar. 2, 2020 [Online]. Available: <https://www.flow3d.com>
- [20] V. Yakhot, S. A. Orszag, S. Thangam, T. B. Gatski, and C. G. Speziale, “Development of turbulence models for shear flows by a double expansion technique,” *Physics of Fluids A*, vol. 4, no. 7, pp. 1510–1520, 1992.
- [21] H. Liu, Z. Qi, and M. Xu, “Numerical simulation of fluid flow and interfacial behavior in three-phase argon-stirred ladles with one plug and dual plugs,” *Steel Research International*, vol. 82, no. 4, pp. 440–458, 2011.
- [22] M.-Y. Zhu, T. Inomoto, I. Sawada, and T.-C. Hsiao, “Fluid flow and mixing phenomena in the ladle stirred by argon through multi-tuyere,” *ISIJ International*, vol. 35, no. 5, pp. 472–479, 1995.
- [23] A. Huang, H. Gu, M. Zhang, N. Wang, T. Wang, and Y. Zou, “Mathematical modeling on erosion characteristics of refining ladle lining with application of purging plug,” *Metallurgical and Materials Transactions B*, vol. 44, no. 3, pp. 744–749, 2013.